

## Supporting information

# Cu<sub>3</sub>P/PAN derived N-Doped Carbon Catalyst with Non-toxic Synthesis for Alkaline Hydrogen Evolution Reaction

*HyoWon Kim<sup>+</sup>, Yongju Lee<sup>+</sup>, DongHoon Song, YongKeun Kwon, Eom-Ji Kim and EunAe Cho\**

Department of Materials Science and Engineering, Korea Advanced Institute of Science and  
Technology (KAIST), 291 Daehak-ro, Yuseong-gu, Daejeon, Republic of Korea

<sup>+</sup>These authors contributed equally

Corresponding Author

EunAe Cho\*: [eacho@kaist.ac.kr](mailto:eacho@kaist.ac.kr)

Supporting information consists of 16 pages, including this page.

There are 15 Figures and 4 Tables.

## List of Figures

Figure S1. Schematic to the synthesis method of  $\text{Cu}_3\text{P}$ ,  $\text{Cu}_3\text{P/N-C}$  and  $\text{N-C}$ .

Figure S2. (a) P:PAN (10:0), (b) P:PAN (9:1), (c) P:PAN (6:4) and (d) P:PAN (0:10). (Small peaks of 41, 45, and 48 observed in all specimens correspond to the  $\text{Cu}_k\beta$  peaks induced in the Cu source of XRD.)

Figure S3. SEM images of (a)  $\text{Cu}_3\text{P}$ , (b)  $\text{Cu}_3\text{P/0.8N-C}$ , (c)  $\text{Cu}_3\text{P/8.8N-C}$  (white circle : N-doped carbon, green circle :  $\text{Cu}_3\text{P}$ ) and (d)  $\text{N-C}$ .

Figure S4. The theoretically-calculated and experimentally-measured amounts of  $\text{H}_2$  gas. (applied current:  $50 \text{ mA/cm}^2$ , temperature:  $26.5 \text{ }^\circ\text{C}$ , electrode rea:  $0.785 \text{ cm}^2$ )

Figure S5. (a) Equivalent circuit models (two-time constant serial model, 2TS) and (b) Nyquist plots for  $\text{Cu}_3\text{P}$ ,  $\text{Cu}_3\text{P/0.8N-C}$ ,  $\text{Cu}_3\text{P/1.9N-C}$ ,  $\text{Cu}_3\text{P/8.8N-C}$  and  $\text{N-C}$  measured at a potential of  $-0.29 \text{ V}_{\text{RHE}}$  in the frequency range from sweep  $10^{-2}$  to  $10^5 \text{ Hz}$  in  $1 \text{ M KOH}$  solution. (solid lines: theoretical fitted curves based on the 2TS model, symbols: experimental data)

Figure S6. Cyclic voltammograms measured at scan rates from  $0.04$  to  $0.5 \text{ V/s}$  (a, c) and corresponding  $j$  vs. scan rates plots (b, d) for  $\text{Cu}_3\text{P/1.9N-C}$  (a, b) and  $\text{Cu}_3\text{P}$  (c, d).

Figure S7. Raman spectra of the  $\text{Cu}_3\text{P/1.9N-C}$  and  $\text{N-C}$ .

Figure S8. XPS spectra of Cu 2p for Cu substrate (Cu film).

Figure S9. XPS spectra of N 1s and C 1s for  $\text{N-C}$ .

Figure S10. Potential-time response (V-t) result of the  $\text{Cu}_3\text{P/1.9N-C}$  in a  $1 \text{ M KOH}$  solution at a HER current density of  $-10 \text{ mA/cm}^2$ .

Figure S11. (a) XRD pattern and (b) SEM image of the  $\text{Cu}_3\text{P/1.9N-C}$  after the HER stability test.

Figure S12. (a) TEM and (b) TEM-EDS mapping images of  $\text{Cu}_3\text{P/1.9N-C}$  after the HER stability test.

Figure S13. XPS spectra of  $\text{Cu}_3\text{P/1.9N-C}$  after the HER stability test.

Figure S14. SEM images of the Cu foam.

Figure S15. (a) HER polarization curves in  $1 \text{ M KOH}$  solution for  $\text{Cu}_3\text{P/N-C@Cu}$  foam with different P/PAN loading amount in  $1 \text{ M KOH}$  solution. (b) XRD pattern for  $\text{Cu}_3\text{P/N-C@Cu}$  foam.

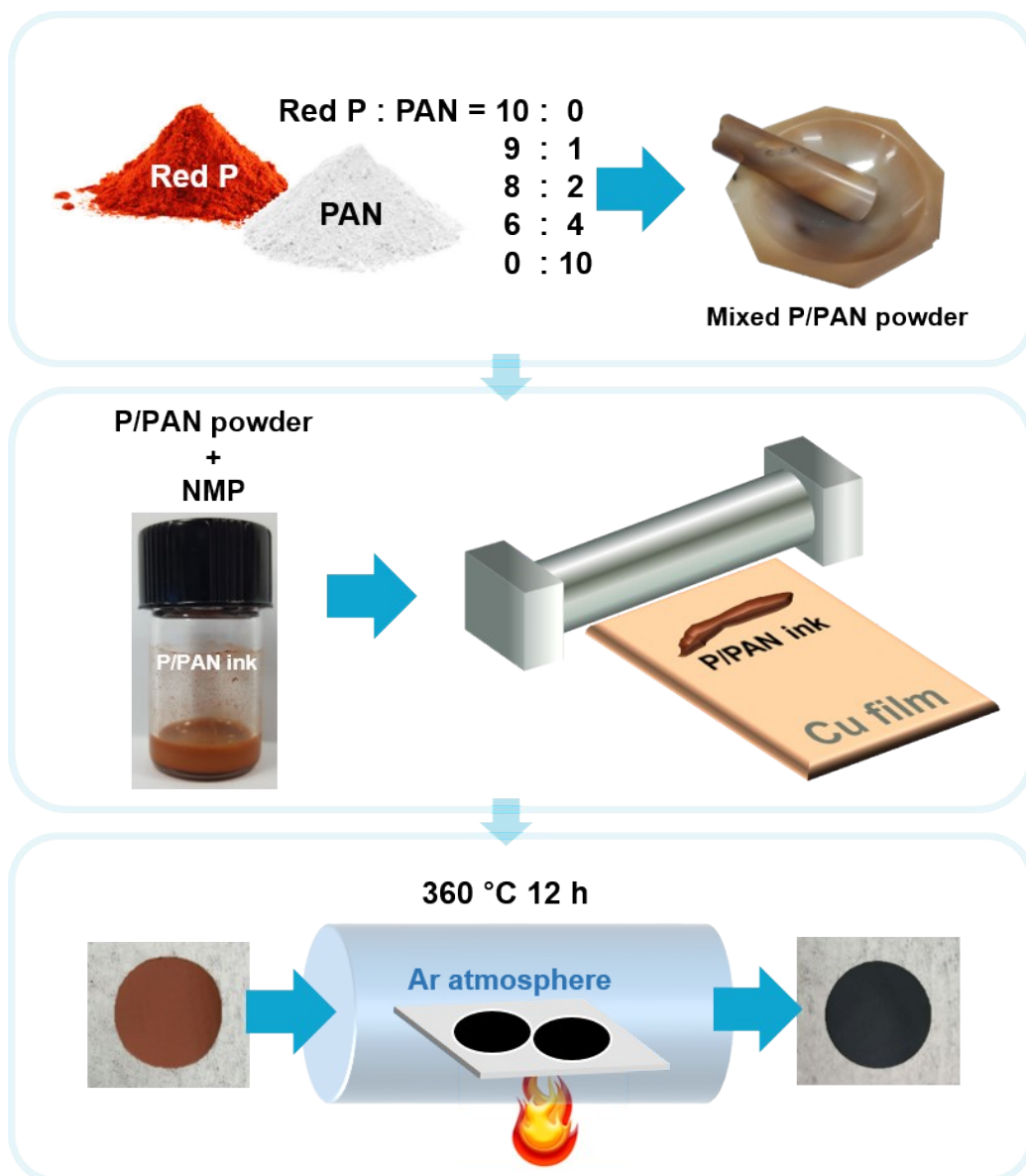
## List of Tables

Table S1. Precursor composition for synthesis to  $\text{Cu}_3\text{P}$ ,  $\text{Cu}_3\text{P/N-C}$  and  $\text{N-C}$ .

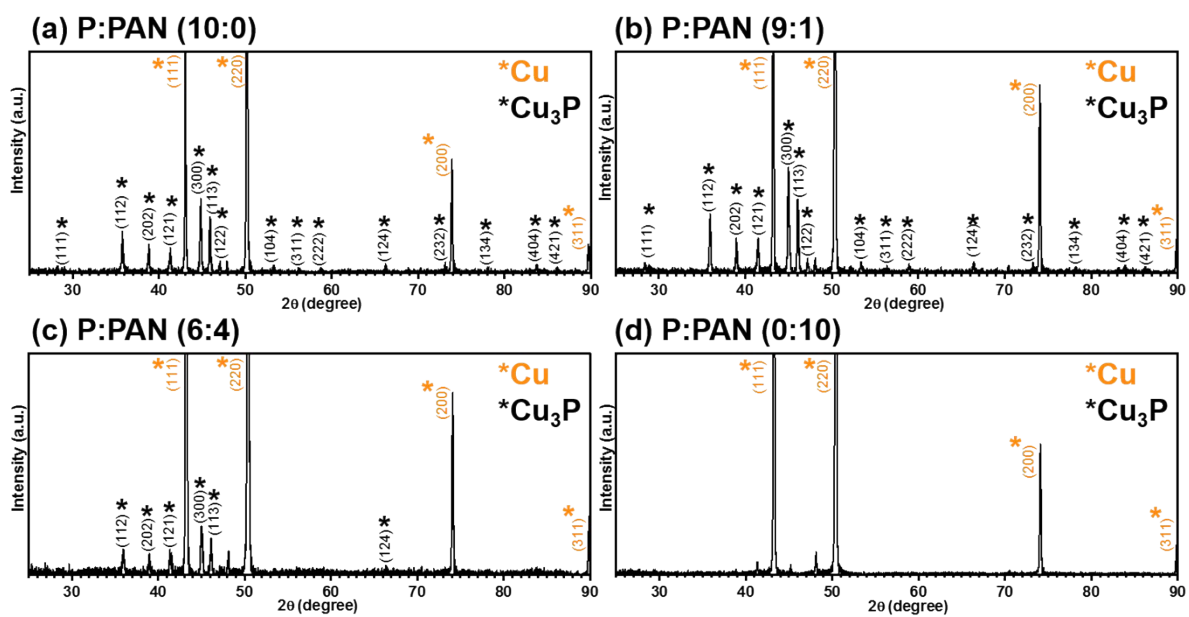
Table S2. Material composition of  $\text{Cu}_3\text{P}$ ,  $\text{Cu}_3\text{P/N-C}$  and  $\text{N-C}$  obtained by XPS analysis.

Table S3. Resistance values obtained from the Nyquist plots fitted based on the 2TS circuit model.

Table S4. Comparison of catalytic activities ( $\text{Cu}_3\text{P}$ ).



**Figure S1.** Schematic to the synthesis method of  $\text{Cu}_3\text{P}$ ,  $\text{Cu}_3\text{P/N-C}$  and  $\text{N-C}$ .



**Figure S2.** XRD patterns of (a) P:PAN (10:0), (b) P:PAN (9:1), (c) P:PAN (6:4) and (d) P:PAN (0:10). (Small peaks of 41, 45, and 48 observed in all specimens correspond to the  $\text{Cu}_k\beta$  peaks induced in the Cu source of XRD.)

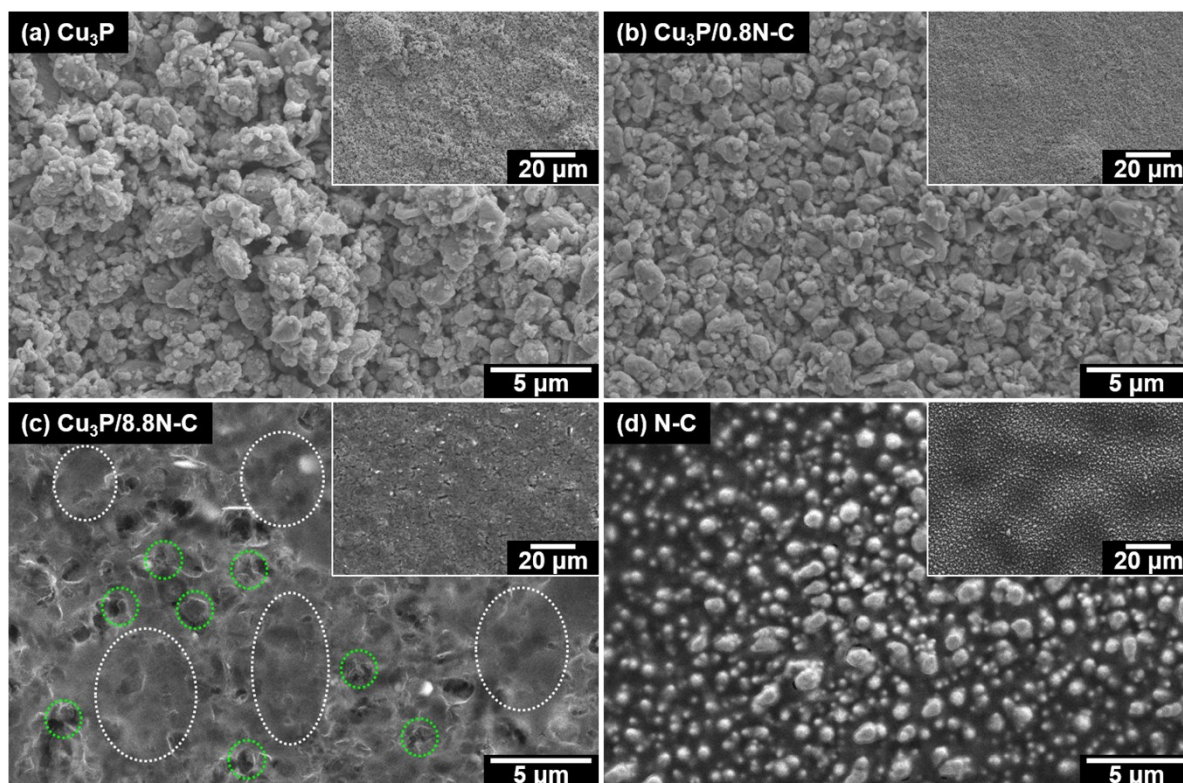


**Figure S3.** SEM images of (a)  $\text{Cu}_3\text{P}$ , (b)  $\text{Cu}_3\text{P}/0.8\text{N-C}$ , (c)  $\text{Cu}_3\text{P}/8.8\text{N-C}$  (white circle : N-doped carbon, green circle :  $\text{Cu}_3\text{P}$ ) and (d) N-C.

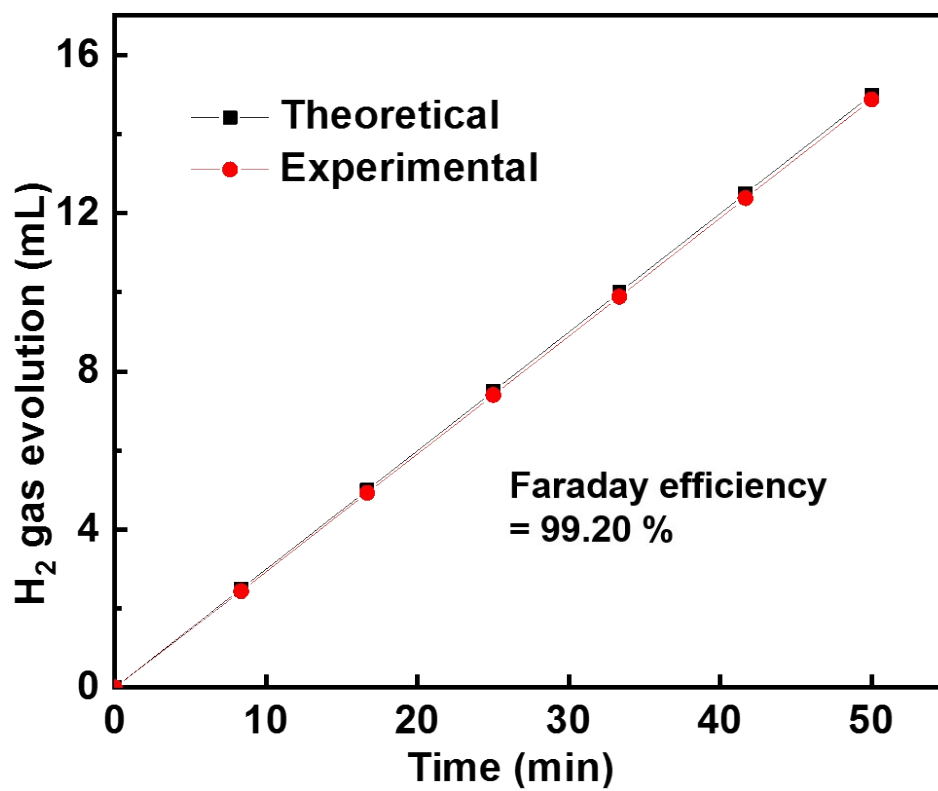


**Figure S4.** The theoretically-calculated and experimentally-measured amounts of H<sub>2</sub> gas. (applied current: 50 mA/cm<sup>2</sup>, temperature: 26.5 °C, electrode rea: 0.785 cm<sup>2</sup>)

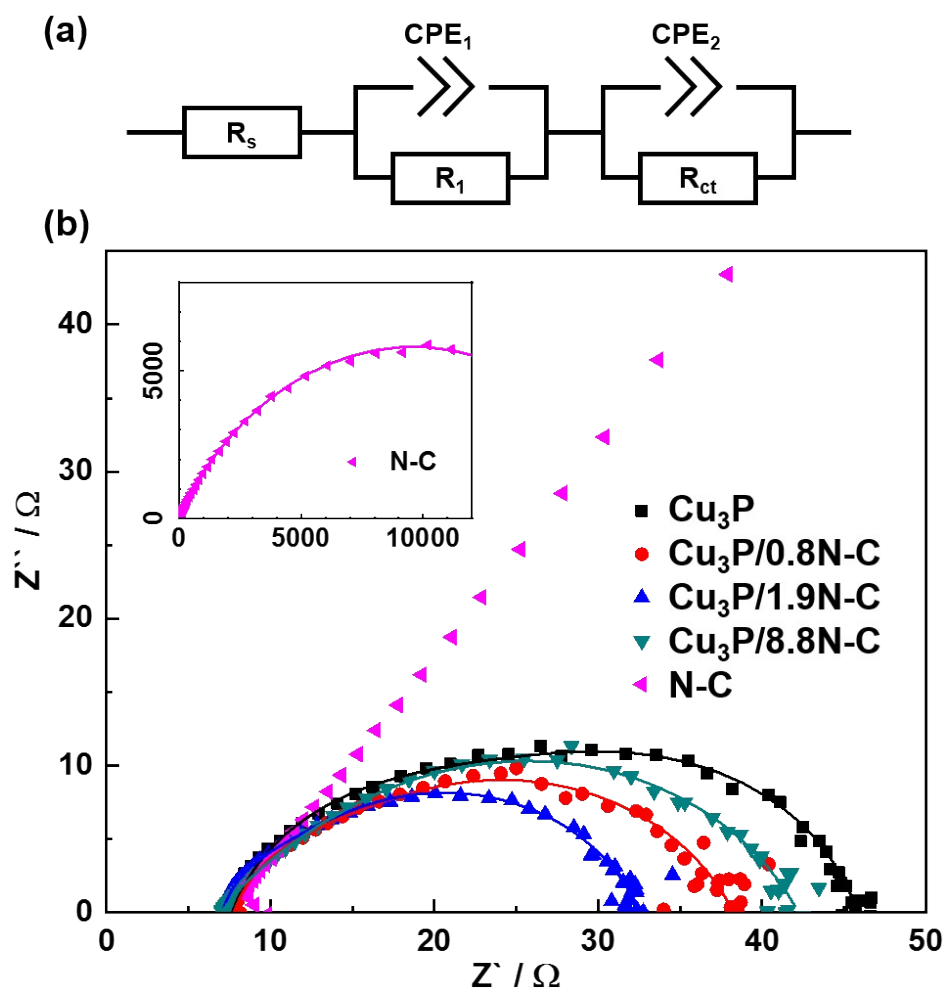


**Figure S5.** (a) Equivalent circuit models (two-time constant serial model, 2TS) and (b) Nyquist plots for  $\text{Cu}_3\text{P}$ ,  $\text{Cu}_3\text{P}/0.8\text{N-C}$ ,  $\text{Cu}_3\text{P}/1.9\text{N-C}$ ,  $\text{Cu}_3\text{P}/8.8\text{N-C}$  and N-C measured at a potential of  $-0.29 \text{ V}_{\text{RHE}}$  in the frequency range from sweep  $10^{-2}$  to  $10^5$  Hz in 1 M KOH solution. (solid lines: theoretical fitted curves based on the 2TS model, symbols: experimental data)

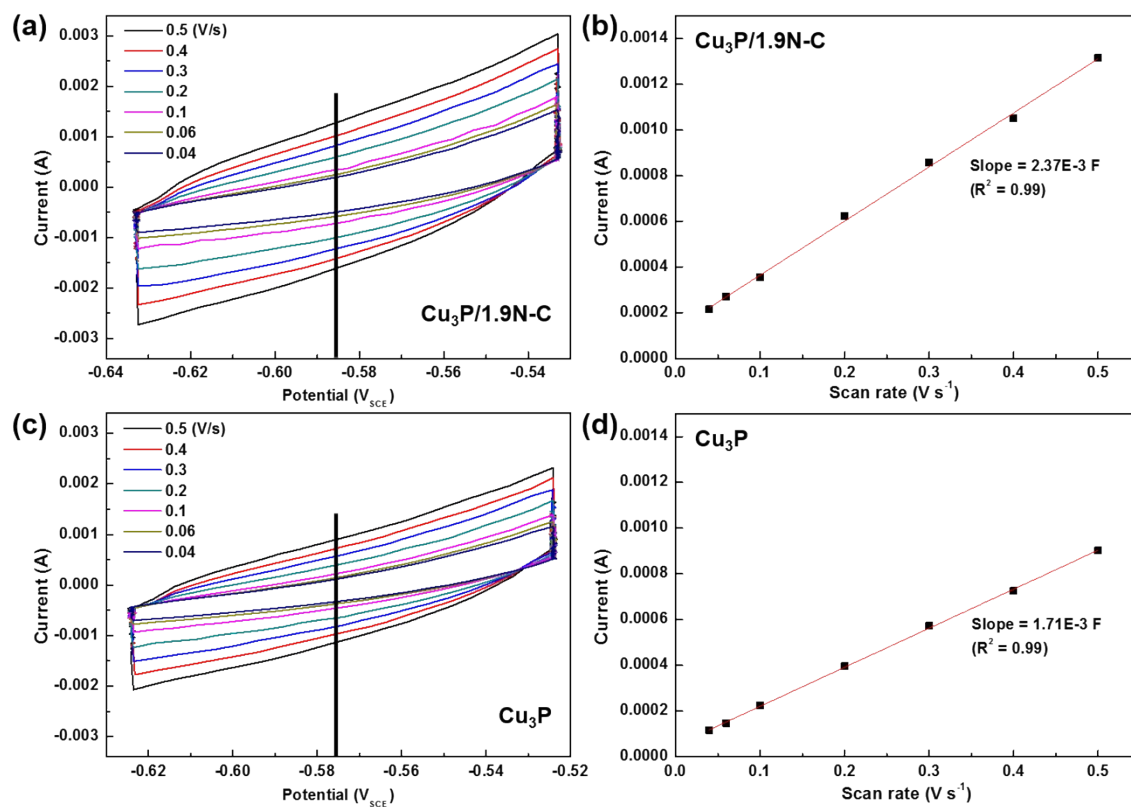


**Figure S6.** Cyclic voltammograms measured at scan rates from 0.04 to 0.5 V/s (a, c) and corresponding  $j$  vs. scan rates plots (b, d) for  $\text{Cu}_3\text{P}/1.9\text{N-C}$  (a, b) and  $\text{Cu}_3\text{P}$  (c, d).

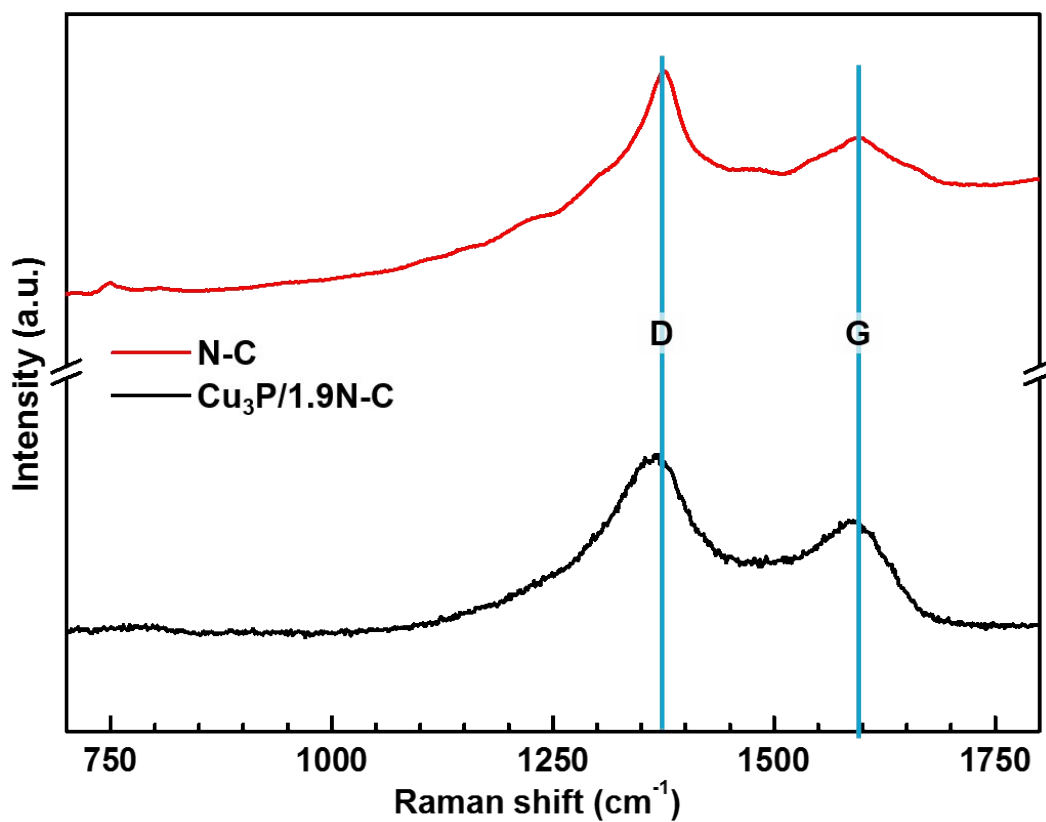


Figure S7. Raman spectra of the  $\text{Cu}_3\text{P}/1.9\text{N-C}$  and N-C.

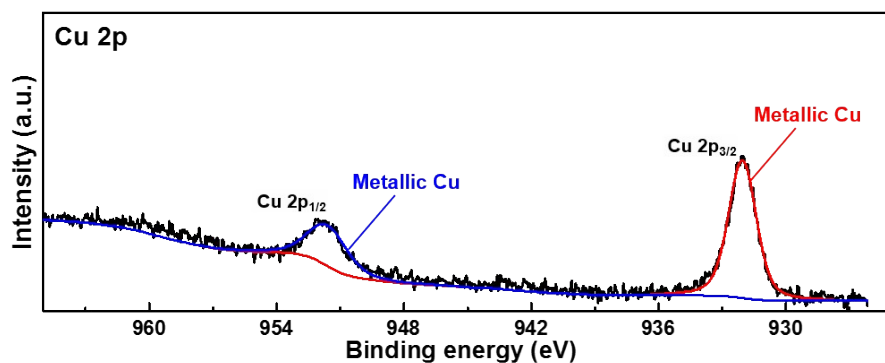
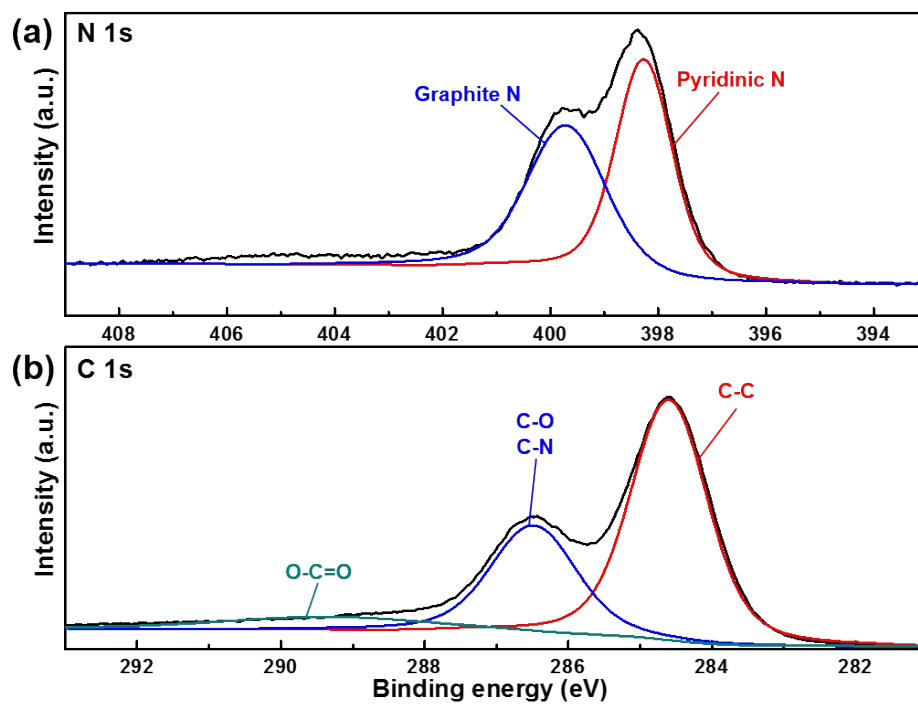
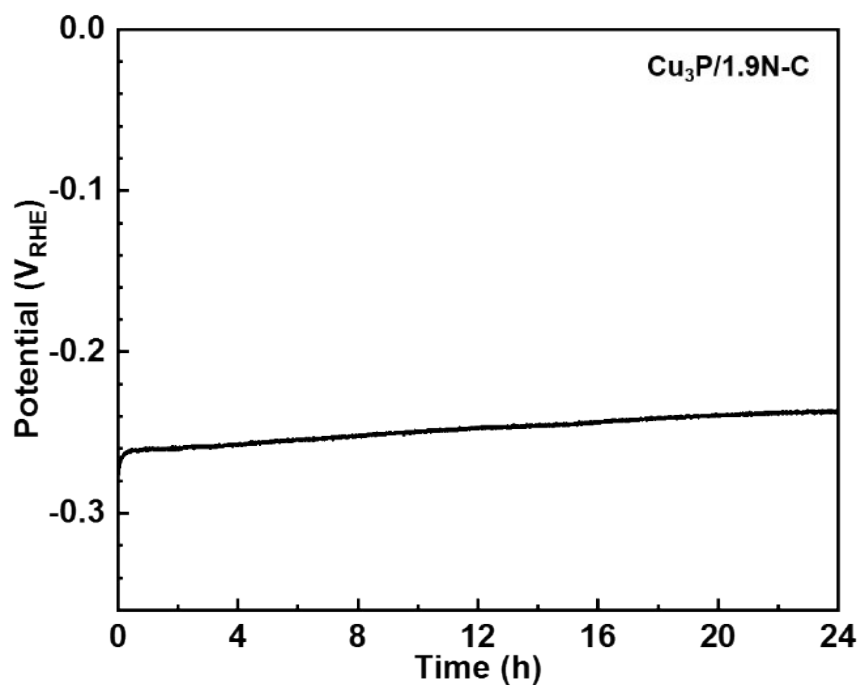


Figure S8. XPS spectra of Cu 2p for Cu substrate (Cu film).



**Figure S9.** XPS spectra of N 1s and C 1s for N-C.



**Figure S10.** Potential-time response (V-t) result of the Cu<sub>3</sub>P/1.9N-C in a 1 M KOH solution at a HER current density of -10 mA/cm<sup>2</sup>.

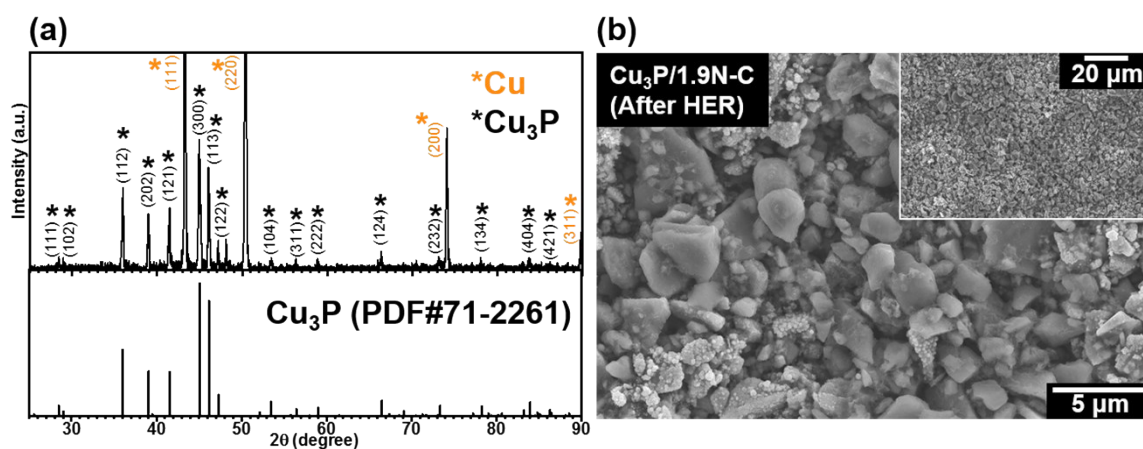


**Figure S11.** (a) XRD pattern and (b) SEM image of the  $\text{Cu}_3\text{P}/1.9\text{N-C}$  after the HER stability test.

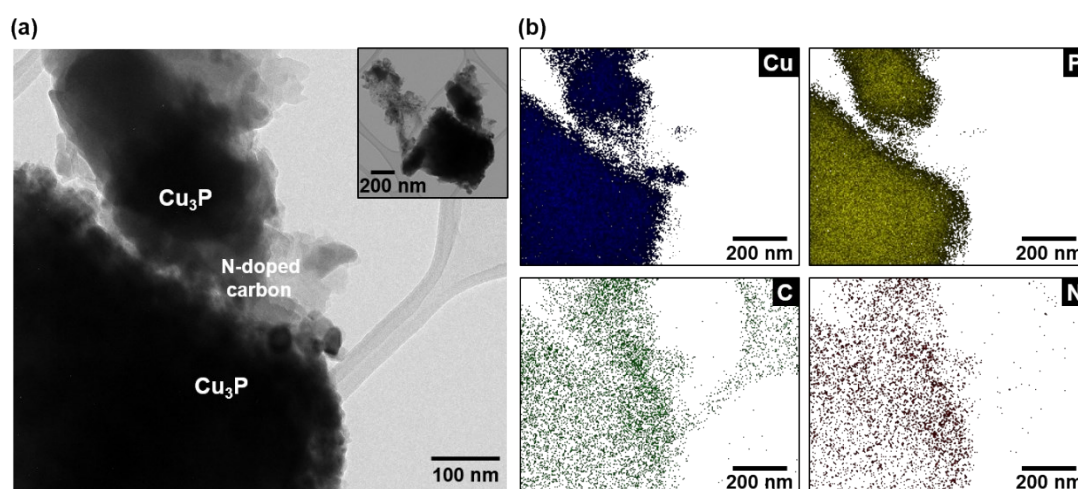


**Figure S12.** (a) TEM and (b) TEM-EDS mapping images of  $\text{Cu}_3\text{P}/1.9\text{N-C}$  after the HER stability test.

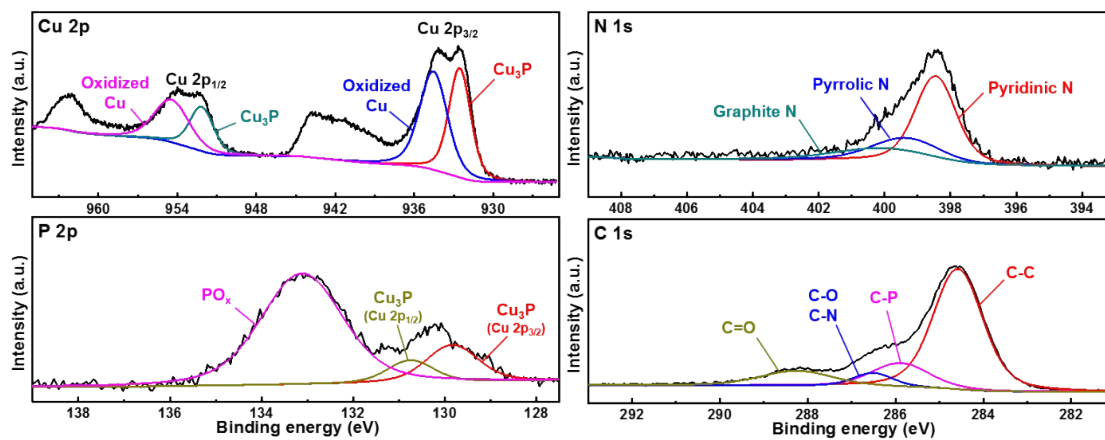


**Figure S13.** XPS spectra of Cu<sub>3</sub>P/1.9N-C after the HER stability test.

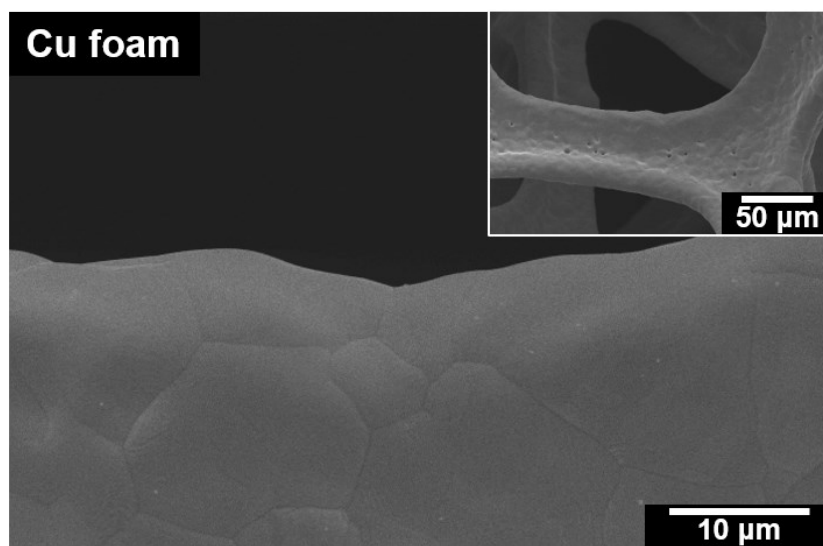


**Figure S14.** SEM images of the Cu foam.

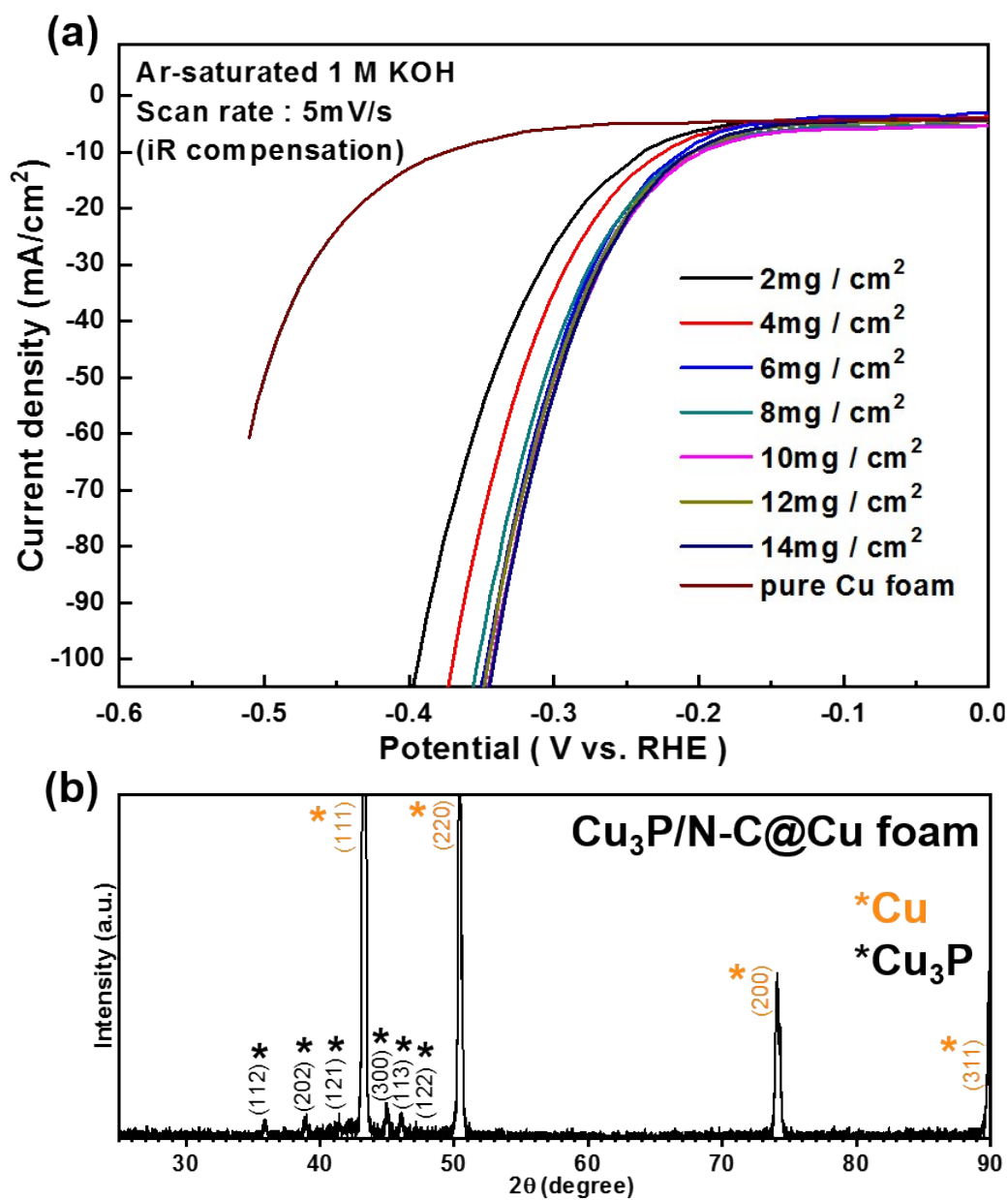


**Figure S15.** (a) HER polarization curves in 1 M KOH solution for Cu<sub>3</sub>P/N-C@Cu foam with different P/PAN loading amount in 1 M KOH solution. (b) XRD pattern for Cu<sub>3</sub>P/N-C@Cu foam.

**Table S1.** Precursor composition for synthesis of Cu<sub>3</sub>P, Cu<sub>3</sub>P/N-C and N-C.

Sample (P: PAN)	P (mg)	PAN (mg)	NMP (uL)	Doctor blade height (Thickness of coated P/PAN ink) (μm)	*Weight of coated P/PAN (Δw, mg/cm <sup>2</sup> )	**Calculated Cu <sub>3</sub> P weight (mg/cm <sup>2</sup> )
<b>P: PAN (10:0)</b>	100	0	105	18.75	0.2863	<b>2.0456</b>
<b>P: PAN (9:1)</b>	90	10	186	25.00	0.3240	<b>2.0833</b>
<b>P: PAN (8:2)</b>	80	20	210	37.50	0.3616	<b>2.0671</b>
<b>P: PAN (6:4)</b>	60	40	350	50.00	0.4746	<b>2.0348</b>
<b>P: PAN (0:10)</b>	0	100	450	62.50	0.3466	-

\* Weight of coated P and PAN (Δw) :

(Measured weight of P/PAN coated Cu film) - (Measured weight of Cu film)

\*\*Cu<sub>3</sub>P weight :

(Ratio of P) × (Δw) × (221.5/31)

Ex) P : PAN = 8 : 2 → Ratio of P = 0.8,

Molar mass → Cu<sub>3</sub>P = 221.5, P = 31.0

**Table S2.** Material composition of Cu<sub>3</sub>P, Cu<sub>3</sub>P/N-C and N-C obtained by XPS analysis.

Sample (P: PAN)	Cu (at%)	P (at%)	C (at%)	N (at%)	**Cu <sub>3</sub> P : C (molar ratio)	Notation
P: PAN (10:0)	72.4	27.6	-	-	-	Cu <sub>3</sub> P
P: PAN (9:1)	61.2	21.0	*16.2	*1.6	1 : 0.8	Cu <sub>3</sub> P/0.8N-C
P: PAN (8:2)	48.8	14.6	31.6	5.0	1 : 1.9	Cu <sub>3</sub> P/1.9N-C
P: PAN (6:4)	19.7	12.5	58.1	9.7	1 : 8.8	Cu <sub>3</sub> P/8.8N-C
P: PAN (0:10)	-	-	86.7	13.3	-	N-C

\*In the case of P: PAN (9:1), the C-to-N ratio is slightly different, most likely due to the XPS fitting margin caused by the low composition of nitrogen.

\*\*Cu<sub>3</sub>P : C = (Cu/3, at%) : (C, at%)

**Table S3.** Resistance values obtained from the Nyquist plots fitted based on the 2TS circuit model.

Sample	R <sub>s</sub> (Ω)	R <sub>ct</sub> (Ω)	R <sub>1</sub> (Ω)
Cu <sub>3</sub> P	7.566	28.791	9.312
Cu <sub>3</sub> P/0.8N-C	7.777	26.560	3.918
Cu <sub>3</sub> P/1.9N-C	7.061	22.911	2.574
Cu <sub>3</sub> P/8.8N-C	7.019	30.930	4.269
N-C	11.062	10.267k	8.419k

\*R<sub>s</sub>: Uncompensated solution resistance

**Table S4.** Comparison of catalytic activities (Cu<sub>3</sub>P).

\*Graph-derived value

Materials	Overpotential of HER in 1 M KOH			Journal	Substrate
	10 mA/cm <sup>2</sup>	50 mA/cm <sup>2</sup>	100 mA/cm <sup>2</sup>		
<b>Cu<sub>3</sub>P/N-C</b>	<b>211.1 mV</b>	<b>301.8 mV</b>	<b>346.4 mV</b>	<b>This work</b>	<b>Cu foam</b>
Cu <sub>3</sub> P nanowires	266 mV	*344 mV	382 mV	<i>ACS Sustainable Chem. Eng.</i> 2018, 6, 380	Cu mesh
Cu <sub>3</sub> P nanoarrays	222 mV (0.1 M KOH)	*364 mV (0.1 M KOH)		<i>ACS Appl. Mater. Interfaces.</i> 2016, 8, 23037	Cu foam
Cu <sub>3</sub> P nanobush	252 mV	*390 mV		<i>ACS Omega</i> 2016, 1, 1367	Cu mesh
NiCuP foam		146 mV	*179 mV	<i>Nanoscale</i> 2017, 9, 4401	Stainless steel
Cu <sub>3</sub> N-Cu <sub>3</sub> P N,P,S doped carbon	68 mV	*130 mV		<i>ChemElectroChem</i> 2020, 7, 289	Ni foam
Cu <sub>3</sub> P-Co <sub>2</sub> P	*95 mV	*175 mV		<i>Nanoscale</i> 2019, 11, 6394	Ni foam
Cu <sub>3</sub> P microsheets	130 mV	*200 mV	*255 mV	<i>Adv. Mater. Interfaces</i> 2016, 3, 1600236	Ni foam
CeO <sub>2</sub> -Cu <sub>3</sub> P		*227 mV	*273 mV	<i>Nanoscale</i> 2018, 10, 2213	Ni foam
Cu <sub>3</sub> P nanosheets	105 mV	*235 mV		<i>ACS Appl. Mater. Interfaces</i> 2017, 9, 2240	Ni foam